https://doi.org/10.31489/2025M3/107-124 *Research article*

Numerical solution of singularly perturbed parabolic differential difference equations

D.B. Huka[1], W.G. Melesse[2], F.W. Gelu[2,*]

[1] *Borana University, Yabello, Ethiopia;*
[2] *Dilla University, Dilla, Ethiopia*
(E-mail: dubura65@gmail.com, gwondwosen12@gmail.com, Fasikag@du.edu.et)

This study presents a computational method for the singularly perturbed parabolic differential difference equations with small negative shifts in convection and reaction terms. To handle the small negative shifts, the Taylor series expansion is applied. Then, the resulting asymptotically equivalent singularly perturbed parabolic convection-diffusion-reaction problem is discretized in the time variable using the implicit Euler technique on a uniform mesh, while the upwind method on a Shishkin mesh is used to discretize the space variable. Almost first-order convergence was achieved by establishing the stability and parameter-uniform convergence of the method. The Richardson extrapolation approach improved the rate of convergence to nearly second-order. Numerical experiments have been carried out in order to support the findings from the theory. The numerical results are presented in tables in terms of maximum absolute errors and graphs. The present results improve the existing methods in the literature. This finding highlights the efficiency of the method, paving the way for its application in other types of singularly perturbed parabolic problems. This method is capable of greatly improving computing performance in a variety of scenarios, which researchers can further explore.

Keywords: singular perturbation problem, differential difference equation, implicit Euler technique, upwind method, Shishkin mesh, parameter-uniform convergence, Richardson extrapolation.

2020 Mathematics Subject Classification: 65M06, 65M12, 65M15, 65M50.

Introduction

In singularly perturbed differential equations, the highest-order derivative term in the differential equation is multiplied by a small perturbation parameter ε $(0 < \varepsilon \ll 1)$. Various numerical solutions have been developed in the literature for a singularly perturbed parabolic problem with general shift arguments in the space variable in [1], retarded terms in [2–4], delay and advances in both reaction terms, differential-difference equations [5–7], functional-differential equations in [8–10]. Some numerical techniques have been devised in [11,12] to solve a singularly perturbed parabolic problem with delay in the reaction terms. Authors in [13–16] developed the numerical solutions for singularly perturbed parabolic differential equation with negative shifts in convection and reaction terms. Recently, authors in [17] considered and solved singularly perturbed partial functional-differential equation. Some numerical methods are devised in [18–20] to solve different types of singularly perturbed parabolic problems.

Therefore, the main purpose of this study is to construct an improved numerical method using implicit Euler method for time direction and upwind method on a Shishkin mesh for space direction together with Richardson extrapolation technique to solve the following singularly perturbed parabolic differential equation with negative shifts in convection and reaction terms

$$\mathcal{L}_{\varepsilon,\mu}u \equiv u_t - \varepsilon u_{xx} + r(x)u_x(x-\mu,t) + s(x)u(x-\mu,t) = f(x,t), \tag{1}$$

*Corresponding author. *E-mail: Fasikag@du.edu.et*
Received: 21 November 2024; *Accepted:* 19 May 2025.

with the initial data

$$u(x,0) = \phi_b(x), \quad x \in \bar{\Omega}, \tag{2}$$

and the interval-boundary data

$$\begin{cases} u(x,t) = \phi_l(x,t), & (x,t) \in [-\mu, 0] \times \Omega_t, \\ u(1,t) = \phi_r(1,t), & t \in \Omega_t, \end{cases} \tag{3}$$

where $(x,t) \in D = \Omega_x \times \Omega_t = (0,1) \times (0,T]$ and $\bar{D} = \bar{\Omega} \times \bar{\Omega}_t = [0,1] \times [0,T]$ for some positive number $T > 0$. The parameter ε is a perturbation parameter such that $0 < \varepsilon \ll 1$, while the positive parameter μ is a small delay parameter (or negative shift) fulfilling $\mu < \varepsilon$. It is assumed that $r(x)$, $s(x)$, $\phi_b(x)$, $\phi_l(x,t)$, $\phi_r(1,t)$ and $f(x,t)$ are sufficiently smooth and bounded to ensure the possibility of a particular solution, and that $s(x)$ satisfies

$$s(x) \geq \beta > 0, \quad x \in \bar{\Omega},$$

for some constant β. Note that (1) contains negative shifts in the convection and reaction terms. When $\mu = 0$, (1) would reduce to the singularly perturbed parabolic differential equation. With a small ε, we observe layers that rely on the value of $r(x)$. We are interested in a related class of problems where both the convection and reaction terms have negative shifts, making it a two-parameter problem. A regular boundary layer appears in the region of the left boundary when $r(x) < 0$, and a boundary layer is located close to the right when $r(x) > 0$.

1 *The continuous problem*

It is reasonable to use the Taylor series approximation for terms involving delay in the case $\mu < \varepsilon$ [21]. Now, approximating $u(x-\mu,t)$ and $u_x(x-\mu,t)$ yields the following

$$\begin{aligned} u(x-\mu,t) &\approx u(x,t) - \mu u_x(x,t) + \frac{\mu^2}{2} u_{xx}(x,t) + O(\mu^3), \\ u_x(x-\mu,t) &\approx u_x(x,t) - \mu u_{xx}(x,t) + O(\mu^2). \end{aligned} \tag{4}$$

Plugging (4) into (1)–(3), we obtain an asymptotically equivalent time-dependent singularly perturbed convection-diffusion-reaction continuous problem of the following form

$$\mathcal{L}_{c_\varepsilon} u \equiv u_t - c_\varepsilon(x) u_{xx} + q(x) u_x + s(x) u(x,t) = f(x,t), \quad (x,t) \in D, \tag{5}$$

with the initial condition

$$u(x,0) = \phi_b(x) \geq 0, \;\; x \in \bar{\Omega}_x, \tag{6}$$

and the boundary conditions

$$u(0,t) = \phi_l(t), \quad u(1,t) = \phi_r(t) \geq 0, \quad t \in \bar{\Omega}_t, \tag{7}$$

where $c_\varepsilon(x) = \varepsilon - \frac{\mu^2}{2} s(x) + \mu r(x)$ and $q(x) = r(x) - \mu s(x)$. With α and β being the lower limits for $r(x)$ and $s(x)$, respectively, we assume that $0 < c_\varepsilon(x) \leq \varepsilon - \frac{\mu^2}{2}\beta + \mu\alpha = c_\varepsilon$. We make the supposition that $q(x) = r(x) - \mu s(x) \geq \gamma > 0$, which suggests the presence of a boundary layer close to $x = 1$ with width $O(\varepsilon)$. The compatibility condition at the corner points, along with the smoothness of $\phi_l(t)$, $\phi_b(x)$, $\phi_r(t)$, can guarantee the existence and uniqueness of the solution for (1)–(3). We now offer bounds on the derivatives of the solution of (1)–(3). To get the bounds, one needs certain information about the solution.

Lemma 1. The solution $u(x,t)$ of (5)–(7) satisfies

$$|u(x,t) - \phi_b(x)| \leq Ct,$$
$$|u(x,t) - \phi_l(t)| \leq C(1-x), \qquad (x,t) \in \bar{D},$$

where C is a constant independent of c_ε.

Setting $c_\varepsilon = 0$ in (5)–(7) gives the reduced problem as

$$\begin{cases} \frac{\partial u^0}{\partial t} + q(x)\frac{\partial u^0}{\partial x} + s(x)u^0(x,t) = f(x,t), & (x,t) \in D, \\ u^0(0,t) = \phi_b(x), & x \in \bar{\Omega}_x, \\ u^0(0,t) = \phi_l(t), \qquad u^0(1,t) \neq \phi_r(t), & t \in \bar{\Omega}_t. \end{cases} \tag{8}$$

The solutions $u(x,t)$ of (5)–(7) and $u^0(x,t)$ of (8) are extremely similar for small values of c_ε. In order to show the bounds of the solution $u(x,t)$ of (5)–(7), we assume $\phi_b(x) = 0$ without compromising generality. Since $\phi_b(x)$ is sufficiently smooth, using the property of norm, we prove the following lemma:

Lemma 2. The bound of the solution $u(x,t)$ to (5)–(7) is given by

$$|u(x,t)| \leq C, \quad (x,t) \in \bar{D}.$$

Proof. From Lemma 1, we have

$$|u(x,t) - \phi_b(x)| \leq Ct.$$

From triangular inequality, we have

$$|u(x,t)| - |\phi_b(x)| \leq |u(x,t) - \phi_b(x)| \leq Ct.$$

This implies that

$$|u(x,t)| \leq Ct + |\phi_b(x)|, \quad (x,t) \in \bar{D}.$$

Since $t \in [0,T]$ and $\phi_b(x)$ is bounded, we have

$$|u(x,t)| \leq C,$$

which is the required result.

The problem (5)–(7) satisfies the following maximum principle.

Lemma 3. Let Θ be a sufficiently smooth function defined on D which satisfies $\Theta(x,t) \geq 0$, $\forall (x,t) \in \partial D$. Then, $\mathcal{L}_{c_\varepsilon}\Theta(x,t) \geq 0$, $(x,t) \in D$ implies that $\Theta(x,t) \geq 0$, $\forall (x,t) \in \bar{D}$.

Proof. See [16].

For the solution of (1), the above maximum principle immediately leads to the stability bound.

Lemma 4. The solution $u(x,t)$ of the continuous (5)–(7) is bounded as

$$|u(x,t)| \leq \max\left\{|\phi_b(x)|, |\phi_l(t)|, |\phi_r(t)|\right\} + \frac{\|f\|}{\beta}.$$

Proof. We define two barrier-functions $\varpi^{\pm}$ as

$$\varpi^{\pm}(x,t) = \max\left\{|\phi_b(x)|, |\phi_l(t)|, |\phi_r(1,t)|\right\} + \frac{\|f\|}{\beta} \pm u(x,t).$$

Evaluating the barrier functions at the initial and boundary conditions, the required bound follows.

Theorem 1. [22] For $0 \le l \le 2,\ 0 \le k \le 3,\ 0 \le l + k \le 3$, the solution $u(x, t)$ of (5)–(7) is bounded by

$$\left|\frac{\partial^{l+k} u(x,t)}{\partial x^l \partial t^k}\right| \le C\left(1 + c_\varepsilon^{-l} e^{-\gamma(1-x)/c_\varepsilon}\right).$$

Stronger bounds should be derived using Shishkin-type decomposition because the bounds on the solution's derivatives are not sufficiently sharp for the proof of uniform convergence. This can be achieved by decomposing the solution u as

$$u = v + w,$$

v is a regular component and w is a singular component. The solution of the non-homogeneous equation is the regular component v

$$\begin{cases} \mathcal{L}_{c_\varepsilon} v(x,t) = f(x,t), & x \in D, \\ v(0,t) = 0, & t \in \Omega_t, \quad v(x,0) = \phi_b(x), \quad x \in \bar{\Omega}_x, \end{cases}$$

and the singular component w represents the homogeneous equation's solution

$$\begin{cases} \mathcal{L}_{c_\varepsilon} w(x,t) = 0, & & x \in D, \\ w(0,t) = 0, & w(1,t) = u(1,t) - v(1,t), & t \in \Omega_t, \\ w(x,0) = 0, & & x \in \bar{\Omega}_x. \end{cases}$$

We can further decompose the regular component v as

$$v = v_0 + c_\varepsilon v_1 + c_\varepsilon^2 v_2,$$

where v_0 is the solution of the reduced problem and v_1 and v_2 are the solution of

$$\begin{cases} (v_1)_t + r(x)(v_1)_x + s(x) v_1 = (v_0)_{xx}, & (x,t) \in D, \\ v_1(x,0) = 0, \quad x \in \bar{\Omega}_x, & v_1(0,t) = 0, \quad t \in \bar{\Omega}_t, \end{cases}$$

and

$$\begin{cases} \mathcal{L}_{c_\varepsilon}(v_2)(x,t) = (v_1)_{xx}, & (x,t) \in D, \\ v_2(x,t) = 0, & (x,t) \in \partial D. \end{cases}$$

Now, we state the bounds for regular and singular components.

Theorem 2. Let v be a regular solution. Then v and its derivative satisfy the bound

$$\left|\frac{\partial^{i+j} v(x,t)}{\partial x^i \partial t^j}\right| \le C(1 + c_\varepsilon^{2-k}), \qquad k = 0, 1, 2.$$

The derivative of regular solution generally bounded as

$$\left|\frac{\partial^{i+j} v(x,t)}{\partial x^i \partial t^j}\right| \le C, \qquad k = 0, 1, 2, 3.$$

Proof. See the proof in [22].

Theorem 3. Let w be the solution of (5)–(7). The bound of w is given by

$$|w(x,t)| \le C e^{-\gamma(1-x)/c_\varepsilon}, \qquad (x,t) \in D.$$

Proof. Considering the barrier functions $\Psi^{\pm}(x,t) = C\left(e^{-\gamma(1-x)/c_\varepsilon}\right)e^t \pm w(x,t),\ (x,t) \in \bar{D}$ and evaluating at the boundaries yields the required result.

Theorem 4. Solution of the singular component w and it derivatives satisfies the bound

$$\left|\frac{\partial^{i+j} w(x,t)}{\partial x^i \partial t^j}\right| \le C c_\varepsilon^{-i} e^{-\gamma(1-x)/c_\varepsilon}, \qquad k = 0,1,2,3.$$

Proof. The proof follows from Theorem 3 and [22].

2 The discrete problem

We use a Shishkin mesh for the space direction and a uniform mesh for the time direction to discretize the problem. The space domain $[0,1]$ is divided into two sub-domains $[0,1-\sigma]$ and $(1-\sigma,1]$, to construct the Shishkin mesh. The transition parameter $1-\sigma$, which divides the coarse and fine regions of the mesh, is determined by taking

$$\sigma = \min\left\{\frac{1}{2}, \frac{\sigma_0 c_\varepsilon}{\gamma}\ln N\right\},$$

where σ_0 denotes a constant that represents the order of the method. We denote the space mesh points by

$$\Omega_x^N = \left\{0 = x_0, x_1, ...x_{N/2} = 1-\sigma, ..., x_N = 1\right\},$$

where

$$x_i = \begin{cases} iH, & i = 0, ...\frac{N}{2}, \\ 1-\sigma + \left(i - \frac{N}{2}\right)h, & i = \frac{N}{2}+1, ...N, \end{cases}$$

and let $N \ge 4$ be a positive even integer. Furthermore, we denote the space mesh size h_i as follows

$$h_i = \begin{cases} H = \frac{2(1-\sigma)}{N}, & i = 1, ..., \frac{N}{2}, \\ h = \frac{2\sigma}{N}, & i = \frac{N}{2}+1, ..., N. \end{cases}$$

To do the analysis, it was assumed that $\sigma = \frac{\sigma_0 c_\varepsilon}{\gamma}\ln N$; if not, N is exponentially larger than ε. It is clear from the above equation that $N^{-1} \le H \le 2N^{-1},\ \ h = \frac{2\sigma_0 c_\varepsilon}{\gamma}N^{-1}\ln N$, and the uniform mesh can be obtained by choosing $\sigma = 1/2$. A uniform mesh with a time step of Δt will be used for the time domain $[0,T]$ so that

$$\Omega_t^M = \left\{t_n = n\Delta t, \ \ n = 0, ...M, \ \ \Delta t = \frac{T}{M}\right\},$$

where M is the number of mesh intervals in the time variable over the interval $[0,T]$. We define the discretized domain $D^{N,\Delta t} = \Omega_x^N \times \Omega_t^M$. Before formulating the numerical method, we introduce the difference operators for a given mesh function $v(x_i,t_n) = v_i^n$ as follows

$$\delta_x^+ v_i^n = \frac{v_{i+1}^n - v_i^n}{h_{i+1}}, \qquad \delta_x^- v_i^n = \frac{v_i^n - v_{i-1}^n}{h_i},$$
$$\delta_x^2 v_i^n = \frac{2(\delta_x^+ v_i^n - \delta_x^- v_i^n)}{\tilde{h}_i} \quad \text{and} \quad \delta_t^- v_i^n = \frac{v_i^n - v_i^{n-1}}{\Delta t},$$

where $\tilde{h}_i$ is defined by $\tilde{h}_i = h_i + h_{i+1},\ \ i = 1, ...N-1$. We now use the upwind method for the space derivative and the implicit Euler method for the time derivative to approximate (5)–(7). The discretisation of (5)–(7) thus assumes the following form:

$$\begin{cases} (\delta_t^- + \mathcal{L}_{c_\varepsilon}^{N,\Delta t})U_i^{n+1} = f_i^{n+1}, & i = 1, ...N-1, \quad n = 0, ..., M-1, \\ U_0^{n+1} = \phi_l(t_{n+1}), & U_N^{n+1} = \phi_r(t_{n+1}), \quad n = 0, ..., M-1, \\ U_i^0 = \phi_b(x_i), & i = 1, ...N-1, \end{cases} \tag{9}$$

where

$$\mathcal{L}_{c_\varepsilon}^{N,\Delta t}U_i^{n+1} = -c_\varepsilon \delta_x^2 U_i^{n+1} + r_i \delta_x^- U_i^{n+1} + s_i U_i^{n+1}.$$

The system of equations that follows is obtained by rearranging the terms in (9)

$$\begin{cases} r_i^- U_{i-1}^{n+1} + r_i^0 U_i^{n+1} + r_i^+ U_{i+1}^{n+1} = g_i^n, & i = 1, ...N-1, \quad n = 0, ...M-1, \\ U_0^{n+1} = \phi_l(t_{n+1}), & U_N^{n+1} = \phi_r(t_{n+1}), \\ U_i^0 = \phi_b(x_i), & i = 1, ...N-1, \end{cases}$$

where the coefficients are given by

$$\begin{cases} r_i^- = \Delta t \left(-\dfrac{2c_\varepsilon}{\tilde{h}_i h_i} - \dfrac{r_i}{h_i} \right), \quad r_i^+ = \Delta t \left(-\dfrac{2c_\varepsilon}{\tilde{h}_i h_{i+1}} \right), \quad r_i^0 = 1 + \Delta t s_i - r_i^- - r_i^+, \\ r_i = r(x_i), \quad s_i = s(x_i), \quad g_i^n = U_i^n + \Delta t f_i^{n+1}. \end{cases}$$

The coefficient matrix of the discrete scheme in (9) gives an $(N-1) \times (N-1)$ linear equation that can be solved uniquely using the Thomas algorithm for the unknowns $U_1, \cdots, U_{N-1}$.

3 Convergence analysis

It can be shown that the discrete maximum principle, which gives the difference operator $(\delta_t^- + \mathcal{L}_{c_\varepsilon}^{N,\Delta t})$ $\varepsilon-$uniform stability, is satisfied by the finite difference operator $(\delta_t^- + \mathcal{L}_{c_\varepsilon}^{N,\Delta t})$ defined in (9).

Lemma 5. Assume that the mesh function $\Psi(x_i, t_n)$ satisfies $\Psi(x_i, t_n) \geq 0$ on $(x_i, t_n) \in D^{N,\Delta t}$. Then, $(\delta_t^- + \mathcal{L}_{c_\varepsilon}^{N,\Delta t})\Psi(x_i, t_n) \geq 0$, $(x_i, t_n) \in D^{N,\Delta t}$ implies that $\Psi(x_i, t_n) \geq 0$ at each point of $(x_i, t_n) \in \bar{D}^{N,\Delta t}$.

The proposed method described in (9) converges ε-uniformly with first-order accuracy in both space and time variables as stated in the following theorem.

Theorem 5. Let U be the numerical solution in (9) and u be the continuous solution in (5)–(7). Therefore, the discrete solution's error $U^{N,\Delta t}$ fulfills the bound

$$|u(x_i, t_n) - U_i^n| \leq C(N^{-1} \ln N + \Delta t), \qquad 1 \leq i \leq N-1.$$

Proof. Readers who are interested may read the proof's details in [23].

The objective of this study was to obtain second-order ε-uniform convergence with respect to both the space and time directions by using the Richardson extrapolation technique to the discrete solution U_i^n of (9). Before introducing this technique, some lemmas are presented as follows:

Lemma 6. On $\bar{D}_x^N = \{x_i\}_0^N$, define the following mesh functions

$$S_i = \prod_{k=1}^{i} \left(1 + \frac{\alpha h_k}{c_\varepsilon} \right)^{-1}, \quad 1 \leq i \leq N,$$

with the usual convention that $S_0 = 1$ for $i = 0$. Then, there exists a positive constant C_1 such that for $i = 1, \cdots, N-1$, we have

$$(\delta_t^- + \mathcal{L}_{c_\varepsilon}^{N,M})S_i \geq \frac{C_1}{c_\varepsilon + \alpha h_i} S_i. \tag{10}$$

Moreover, for $N/2+1 \le i \le N-1$ and constant C_2, we have

$$(\delta_t^- + \mathcal{L}_{c_\varepsilon}^{N,M})S_i \ge C_2 c_\varepsilon^{-1} S_i. \tag{11}$$

Proof. Now, $S_i - S_{i-1} = \frac{\alpha h_i}{c_\varepsilon} S_{i-1}$. So, we have

$$\begin{aligned}(\delta_t^- + \mathcal{L}_{c_\varepsilon}^{N,M})S_i &= -\frac{2\alpha}{(h_i+h_{i+1})}(S_i - S_{i-1}) + \alpha\frac{\alpha}{c_\varepsilon}S_{i-1} + \beta S_i \\ &\ge \frac{\alpha}{c_\varepsilon}S_{i-1}\left[r_i - \frac{2\alpha h_i}{(h_i+h_{i+1})}\right] \\ &\ge \frac{C\alpha}{c_\varepsilon + \alpha h_i}S_i, \qquad 1 \le i \le N-1.\end{aligned}$$

As a result, since $h/c_\varepsilon < 4/\gamma$, (10) is proven, and (11) is a straightforward consequence of it.

Lemma 7. The following inequality is satisfied by the mesh function S_i

$$e^{-\gamma(1-x_i)/c_\varepsilon} \le \prod_{k=i+1}^{N}\left(1+\frac{\alpha h_k}{c_\varepsilon}\right)^{-1} = S_i, \qquad 0 \le i \le N, \tag{12}$$

and on Shishkin mesh, the mesh function $S_{c_\varepsilon,i}$ also satisfies the following inequality

$$\prod_{k=i+1}^{N}\left(1+\frac{\alpha h_k}{c_\varepsilon}\right)^{-1} \le CN^{-4(1-i/N)}, \qquad N/2 \le i \le N-1. \tag{13}$$

We solve the discrete scheme in (9) on the fine mesh $D^{2N,\Delta t/2} = \bar{\Omega}_x^{2N} \times \bar{\Omega}_t^{\Delta t/2}$ with $2N$ mesh intervals in the space direction and $2M$ mesh intervals in the time direction, where $\bar{\Omega}_x^{2N}$ is a piecewise uniform Shishkin mesh with the same transition point $1-\sigma$ as Ω_x^N. This improves the accuracy of the numerical solution $U^{N,\Delta t}$ using the Richardson extrapolation technique. Actually, by dividing each mesh interval of Ω_x^N in half, the discrete domain $\bar{\Omega}_x^{2N}$ may be produced. It is evident from this construction that $D^{N,\Delta t} = (x_i, t_n) \subset D^{2N,\Delta t/2} = \{(\tilde{x}_i, \tilde{t}_n)\}$. Thus, the suitable mesh widths in $D^{2N,\Delta t/2}$ may be obtained using

$$\tilde{x}_i - \tilde{x}_{i-1} = \begin{cases} H/2, & \text{for } \tilde{x}_i \in \bar{\Omega}_x^{2N} \cap [0, 1-\sigma], \\ h/2, & \text{for } \tilde{x}_i \in \bar{\Omega}_x^{2N} \cap [1-\sigma, 1], \end{cases}$$

and $\tilde{t}_n - \tilde{t}_{n-1} = \Delta t/2$, $\tilde{t}_n \in \bar{\Omega}_t^{\Delta t/2}$. On the mesh $D^{N,\Delta t}$, let $U(x_i, t_n)$ represent the numerical solution of the discrete scheme in (9). Thus, using Theorem 5, one may write on $(x_i, t_n) \in D^{N,\Delta t}$

$$\begin{aligned} U^{N,\Delta t}(x_i,t_n) - u(x_i,t_n) &= C(N^{-1}\ln N + \Delta t) + R_{N,\Delta t}(x_i,t_n) \\ &= C(N^{-1}(\gamma\sigma/\sigma_0 c_\varepsilon) + \Delta t) + R_{N,\Delta t}(x_i,t_n), \end{aligned} \tag{14}$$

where C is fixed constant and the remainder term $R_{N,\Delta t}(x_i,t_n)$ is $o(N^{-1}\ln N + \Delta t)$. Similarly, if $\tilde{U}^{2N,\Delta t/2}$ is the solution of the discrete (14) for $(\tilde{x}_i, \tilde{t}_n) \in D^{2N,\Delta t/2}$, then

$$\tilde{U}^{2N,\Delta t/2}(\tilde{x}_i,\tilde{t}_n) - \tilde{u}(\tilde{x}_i,\tilde{t}_n) = C\bigg((2N)^{-1}(\sigma\gamma/\sigma_0 c_\varepsilon) + \Delta t/2\bigg) + R_{2N,\Delta t/2}(x_i,t_n), \tag{15}$$

by considering the fact that $\tilde{U}(\tilde{x}_i, \tilde{t}_n)$ is obtained using the same transition point $1-\sigma$ and the remainder term $R_{2N,\Delta t/2}(x_i,t_n)$ is $o(N^{-1}\ln N + \Delta t)$. Now, eliminating the terms $O(N^{-1})$ and $O(\Delta t)$ from (14) and (15) leads to the following approximation

$$\begin{aligned} u_i^n - \bigg(2\tilde{U}^{2N,\Delta t/2}(x_i,t_n) - U^{N,\Delta t}(x_i,t_n)\bigg) &= -2R_{2N,\Delta t/2}(x_i,t_n) + R_{N,\Delta t}(x_i,t_n) \\ &= o(N^{-1}\ln N + \Delta t), \quad (x_i,t_n) \in \bar{D}^{N,\Delta t}. \end{aligned}$$

Therefore, we will utilize the following extrapolation formula:

$$U_{extp}^{N,\Delta t}(x_i,t_n)=2\tilde{U}^{2N,\Delta t/2}(x_i,t_n)-U^{N,\Delta t}(x_i,t_n),\quad (x_i,t_n)\in\bar{D}^{N,M}, \tag{16}$$

to get a more accurate predicted numerical solution for $u(x,t)$. After extrapolating $U^{N,\Delta t}$, we obtain the estimate of the nodal error $|u(x_i,t_n)-U_{textp}^{N,\Delta t}(x_i,t_n)|$ by splitting the solution $U^{N,\Delta t}$ on the mesh $\bar{D}_{\sigma}^{N,M}$ into the sum

$$U^{N,\Delta t}=V^{N,\Delta t}+W^{N,\Delta t},$$

where the following discrete problems are solved by the regular component $V^{N,\Delta t}$ and the singular component $W^{N,\Delta t}$, respectively

$$\begin{cases}\mathcal{L}_{c_\varepsilon}^{N,\Delta t}V^{N,\Delta t}=f, \quad D^{N,\Delta t}, \quad V^{N,\Delta t}=v, \quad \partial D^{N,\Delta t},\\ \mathcal{L}_{c_\varepsilon}^{N,\Delta t}W^{N,\Delta t}=0, \quad D^{N,\Delta t}, \quad W^{N,\Delta t}=w, \quad \partial D^{N,\Delta t}.\end{cases} \tag{17}$$

Likewise, on the fine mesh $\bar{D}^{2N,\Delta t/2}$, we decomposed the solution $\tilde{U}^{2N,\Delta t/2}$ into the regular component $\tilde{V}^{2N,\Delta t/2}$ and the singular component $\tilde{W}^{2N,\Delta t/2}$ given by

$$\tilde{U}^{2N,\Delta t/2}=\tilde{V}^{2N,\Delta t/2}+\tilde{W}^{2N,\Delta t/2}.$$

The error can then be expressed using the form given below.

$$\begin{aligned}U^{N,\Delta t}-u&=\left(V^{N,\Delta t}-v\right)+\left(W^{N,\Delta t}-w\right),\\ \tilde{U}^{2N,\Delta t/2}-u&=\left(\tilde{V}^{2N,\Delta t/2}-v\right)+\left(\tilde{W}^{2N,\Delta t/2}-w\right).\end{aligned}$$

Lemma 8. Let $c_\varepsilon\le N^{-1}$. Then, the error associated with the smooth component $V^{N,\Delta t}$ after extrapolation fulfills the bound

$$|v(x_i,t_n)-V_{extp}^{N,\Delta t}(x_i,t_n)|\le C\left(N^{-2}+\Delta t^2\right),\qquad 1\le i\le N-1.$$

Proof. It may be deduced from the extrapolation formula (15), Lemma 7, and (17) that

$$\begin{aligned}v(x_i,t_n)-V_{extp}^{N,\Delta t}(x_i,t_n)&=v(x_i,t_n)-\left(2\tilde{V}^{2N,\Delta t/2}(x_i,t_n)-V^{N,\Delta t}(x_i,t_n)\right)\\ &=-2\left(\tilde{V}^{2N,\Delta t/2}-v\right)(x_i,t_n)+\left(V^{N,\Delta t}-v\right)(x_i,t_n)\\ &=O\left(N^{-2}+\Delta t^2\right),\end{aligned}$$

from which the expected result is obtained.

Lemma 9. The extrapolated error for the layer component $W^{N,\Delta t}$ satisfies

$$|w(x_i,t_n)-W_{extp}^{N,\Delta t}(x_i,t_n)|\le C(N^{-2}+\Delta t^2),\qquad 1\le i\le N/2.$$

Proof. Assume $1\le i\le N/2$. This allows us to demonstrate, using (13) and the argument provided in [24] over $\bar{D}^{N,M}$, that

$$|W^{N,\Delta t}(x_i,t_n)|\le C\prod_{j=i+1}^{N}\left(1+\frac{\alpha h_j}{c_\varepsilon}\right)^{-1}\le CN^{-2}.$$

We then derive $|w(x_i,t_n)|\le CN^{-2}$ from (12) and Theorem 3. So, we have

$$|W^{N,\Delta t}-w(x_i,t_n)|\le C(N^{-2}+\Delta t^2).$$

In the same way, $|\tilde{W}^{N,\Delta t}-w(x_i,t_n)|\le C(N^{-2}+\Delta t^2)$. The extrapolation formula (16) is used to acquire a required extrapolated error bound.

Lemma 10. Once the layer component $W^{N,\Delta t}$ has been extrapolated, the error associated with it satisfy

$$\left| w(x_i,t_n) - W^{N,\Delta t}_{extp}(x_i,t_n) \right| \le C\left(N^{-2}\ln^2 N + \Delta t^2\right), \qquad N/2 < i < N.$$

Proof. See [23].

The following theorem is the main finding of this study.

Theorem 6. Let $c_\varepsilon \le N^{-1}$. Suppose u be the continuous problem solution and $U^{N,\Delta t}_{textp}$ be the solution that was obtained by solving the discrete problem using the Richardson extrapolation strategy. Consequently, the error connected to the solution $U^{N,\Delta t}_{textp}$ meets

$$\left| u(x_i,t_n) - U^{N,\Delta t}_{extp}(x_i,t_n) \right| \le C\left(N^{-2}\ln^2 N + \Delta t^2\right), \qquad 1 \le i \le N-1. \tag{18}$$

Proof. For each $(x_i,t_n) \in \bar{D}^{N,\Delta t}$, we have

$$u(x_i,t_n) - U^{N,\Delta t}_{extp} = \left(v(x_i,t_n) - V^{N,\Delta t}_{extp}\right) + \left(w(x_i,t_n) - W^{N,\Delta t}_{extp}\right).$$

Thus, when Lemma 8 for the regular component and Lemmas 9 and 10 for the singular component are combined, the result (18) is obtained immediately.

4 Numerical computations and discussions

In order to verify the performance of the present method with the theoretical findings discussed in the preceding parts, we do numerical calculations in this section.

Example 1. Consider a singularly perturbed parabolic problem [16]:

$$\begin{cases} \frac{\partial u}{\partial t} - \varepsilon\frac{\partial^2 u}{\partial x^2} + (2-x^2)\frac{\partial u}{\partial x} + (x^2+1+\cos(\pi x))u = 10t^2x(1-x)e^{-t}, & (x,t)\in[0,1]\times[0,1], \\ \begin{cases} u(x,0)=0, & 0\le x\le 1, \\ u(0,t)=0, \quad u(1,t)=0, & 0\le t\le 1. \end{cases} \end{cases}$$

Example 2. Consider a singularly perturbed parabolic problem [16]:

$$\begin{cases} \frac{\partial u}{\partial t} - \varepsilon\frac{\partial^2 u}{\partial x^2} + (2-x^2)\frac{\partial u(x-\mu,t)}{\partial x} + (x^2+1+\cos(\pi x))u(x-\mu,t) = 10t^2(1-x)e^{-t}, (x,t)\in[0,1]\times[0,1], \\ \begin{cases} u(x,0)=0, & 0\le x\le 1, \\ u(x,t)=0, \ \ \mu\le x\le 0,\ 0\le t\le 1, \quad u(1,t)=0, & 0\le t\le 1. \end{cases} \end{cases}$$

Example 3. Consider a singularly perturbed parabolic problem [22]:

$$\begin{cases} \frac{\partial u}{\partial t} - \varepsilon\frac{\partial^2 u}{\partial x^2} + \frac{\partial u}{\partial x} + (1+x^2)u = 50(x(1-x))^3, & (x,t)\in[0,1]\times[0,2], \\ \begin{cases} u(x,0)=0, & 0\le x\le 1, \\ u(0,t)=0, \quad u(1,t)=0, & 0\le t\le 2. \end{cases} \end{cases}$$

Since there are no exact solutions for the examples, we estimate the maximum absolute errors for each (ε,μ) using the double mesh principle via the following formula:

$$e^{N,\Delta t}_{\varepsilon,\mu} = \max_{0\le i\le N; 0\le j\le M} \left| U^{N,\Delta t}(x_i,t_n) - U^{2N,\Delta t/2}(x_i,t_n) \right|,$$

before extrapolation and after extrapolation, we use the formula

$$(e_{\varepsilon,\mu}^{N,\Delta t})^{extr} = \max_{0\le i\le N; 0\le j\le M} \left|(U^{N,\Delta t})^{extr}(x_i,t_n) - (U^{2N,\Delta t/2})^{extr}(x_i,t_n)\right|,$$

where $U^{N,\Delta t}(x_i,t_n)$ is the numerical solution with $(N,\Delta t)$ mesh points and $U^{2N,\Delta t/2}(x_i,t_n)$ is the numerical solution at the finer mesh with $(2N,\Delta t/2)$ mesh points before extrapolation. The numerical solutions after extrapolation are $(U^{N,\Delta t})^{extr}(x_i,t_n)$ using the mesh points $(N,\Delta t)$ with mesh sizes h_i and Δt and $(U^{2N,\Delta t/2})^{extr}(x_i,t_n)$ using the mesh points $(2N,\Delta t/2)$ with mesh sizes $\frac{h_i}{2}$ and $\frac{\Delta t}{2}$. The (ε,μ)-maximum errors before and after extrapolations were calculated using the following formulas, respectively

$$e^{N,\Delta t} = \max_{\varepsilon,\mu} e_{\varepsilon,\mu}^{N,\Delta t} \quad \text{and} \quad (e^{N,\Delta t})^{extr} = \max_{\varepsilon,\mu} (e_{\varepsilon,\mu}^{N,\Delta t})^{extr}.$$

Furthermore, we compute the numerical rate of convergence before and after extrapolation with the following formulas, respectively

$$\rho_{\varepsilon,\mu}^{N,\Delta t} = \log_2\left(\frac{e_{\varepsilon,\mu}^{N,\Delta t}}{e_{\varepsilon,\mu}^{2N,\Delta t/2}}\right) \quad \text{and} \quad (\rho_{\varepsilon,\mu}^{N,\Delta t})^{extr} = \log_2\left(\frac{(e_{\varepsilon,\mu}^{N,\Delta t})^{extr}}{(e_{\varepsilon,\mu}^{2N,\Delta t/2})^{extr}}\right).$$

The (ε,μ)-maximum rates of convergence before and after extrapolations were calculated using the following formulas, respectively

$$\rho^{N,\Delta t} = \max_{\varepsilon,\mu} \rho_{\varepsilon,\mu}^{N,\Delta t} \quad \text{and} \quad \rho_{extr}^{N,\Delta t} = \max_{\varepsilon,\mu} (\rho_{\varepsilon,\mu}^{N,\Delta t})^{extr}.$$

Table 1

Computation of maximum point-wise errors and rate of convergence for $N = \frac{1}{\Delta t}, \mu = 0$, Example 1

$\varepsilon \downarrow$	Extrapolation	$N = 32$	64	128	256	512
10^{-6}	Before Extrapolation	8.5069e-03	5.1386e-03	2.8624e-03	1.5340e-03	8.0921e-04
	Rate	0.7273	0.8442	0.8999	0.9227	
	After Extrapolation	6.4391e-04	2.1982e-04	6.5090e-05	1.8622e-05	5.8390e-06
	Rate	1.5505	1.7558	1.8054	1.6732	
10^{-8}	Before Extrapolation	8.5068e-03	5.1384e-03	2.8621e-03	1.5337e-03	8.0896e-04
	Rate	0.7273	0.8442	0.9001	0.9229	
	After Extrapolation	6.4325e-04	2.1923e-04	6.4592e-05	1.8006e-05	5.2361e-06
	Rate	1.5529	1.7630	1.8429	1.7819	
10^{-10}	Before Extrapolation	8.5068e-03	5.1384e-03	2.8621e-03	1.5337e-03	8.0896e-04
	Rate	0.7273	0.8442	0.9001	0.9229	
	After Extrapolation	6.4325e-04	2.1923e-04	6.4584e-05	1.8001e-05	5.2298e-06
	Rate	1.5529	1.7632	1.8431	1.7832	
10^{-12}	Before Extrapolation	8.5068e-03	5.1384e-03	2.8621e-03	1.5337e-03	8.0896e-04
	Rate	0.7273	0.8442	0.9001	0.9229	
	After Extrapolation	6.4325e-04	2.1923e-04	6.4584e-05	1.8001e-05	5.2298e-06
	Rate	1.5529	1.7632	1.8431	1.7832	
$e^{N,\Delta t}$	Before Extrapolation	8.5069e-03	5.1386e-03	2.8624e-03	1.5340e-03	8.0921e-04
$\rho^{N,\Delta t}$	Rate	0.7273	0.8442	0.8999	0.9227	
$e_{extr}^{N,\Delta t}$	After Extrapolation	6.4391e-04	2.1982e-04	6.5090e-05	1.8622e-05	5.8390e-06
$\rho_{extr}^{N,\Delta t}$	Rate	1.5505	1.7558	1.8054	1.6732	

Table 2

Computation of maximum point-wise errors and rate of convergence for $N = \frac{1}{\Delta t}$, $\mu = 0.3\varepsilon$, Example 2

$\varepsilon \downarrow$	Extrapolation	$N = 32$	64	128	256	512
10^{-6}	Before Extrapolation	1.9445e-02	1.0633e-02	6.0314e-03	3.2579e-03	1.7222e-03
	Rate	0.8709	0.8180	0.8886	0.9197	
	After Extrapolation	1.6756e-03	6.1162e-04	1.9601e-04	7.6087e-05	2.8981e-05
	Rate	1.4540	1.6417	1.3652	1.3925	
10^{-8}	Before Extrapolation	1.9445e-02	1.0633e-02	6.0307e-03	3.2572e-03	1.7215e-03
	Rate	0.8709	0.8182	0.8887	0.9200	
	After Extrapolation	1.6737e-03	6.0967e-04	1.9661e-04	7.6346e-05	2.8879e-05
	Rate	1.4569	1.6327	1.3647	1.4025	
10^{-10}	Before Extrapolation	1.9445e-02	1.0633e-02	6.0307e-03	3.2572e-03	1.7215e-03
	Rate	0.8709	0.8182	0.8887	0.9200	
	After Extrapolation	1.6737e-03	6.0965e-04	1.9662e-04	7.6352e-05	2.8886e-05
	Rate	1.4570	1.6326	1.3647	1.4023	
10^{-12}	Before Extrapolation	1.9445e-02	1.0633e-02	6.0307e-03	3.2572e-03	1.7215e-03
	Rate	0.8709	0.8182	0.8887	0.9200	
	After Extrapolation	1.6737e-03	6.0965e-04	1.9662e-04	7.6352e-05	2.8886e-05
	Rate	1.4570	1.6326	1.3647	1.4023	
$e^{N,\Delta t}$	Before Extrapolation	1.9445e-02	1.0633e-02	6.0314e-03	3.2579e-03	1.7222e-03
$\rho^{N,\Delta t}$	Rate	0.8709	0.8180	0.8886	0.9197	
$e^{N,\Delta t}_{extr}$	After Extrapolation	1.6756e-03	6.1162e-04	1.9662e-04	7.6352e-05	2.8981e-05
$\rho^{N,\Delta t}_{extr}$	Rate	1.4540	1.6372	1.3647	1.3976	

Table 3

Comparison using $N = \frac{1}{\Delta t}$, $\mu = 0.3\varepsilon$ for Example 2

Extrapolation	$N = 16$	32	64	128
Present method				
Before Extrapolation	3.4791e-02	1.9445e-02	1.0633e-02	6.0314e-03
Rate	0.8393	0.8709	0.8180	
After Extrapolation	4.0244e-03	1.6756e-03	6.1162e-04	1.9662e-04
Rate	1.2641	1.4540	1.6372	
Result in [16]				
Before Extrapolation	1.3567e-02	7.7535e-03	4.1434e-03	2.5115e-03
Rate	0.8072	0.9040	0.7223	
After Extrapolation	7.5907e-03	2.3678e-03	8.2018e-04	2.5398e-04
Rate	1.6807	1.5295	1.6912	

Table 4

Computation of maximum point-wise errors and rate of convergenceat $\mu = 0$ for Example 3 with [22]

$\varepsilon \downarrow$	Extrapolation	$N = 32$ $\Delta t = 0.05$	64 $\frac{0.05}{2}$	128 $\frac{0.05}{2^2}$	256 $\frac{0.05}{2^3}$	512 $\frac{0.05}{2^4}$
2^{-6}	Before Extrapolation	1.2677e-2	7.4327e-3	4.0929e-3	2.1883e-3	1.1609e-3
	Rate	0.7703	0.8608	0.9033	0.9146	
	After Extrapolation	2.4529e-3	8.7923e-4	2.7423e-4	8.0145e-5	2.2686e-5
	Rate	1.4802	1.6809	1.7747	1.8208	
2^{-10}	Before Extrapolation	1.4598e-2	8.9967e-3	5.1615e-3	2.8253e-3	1.5371e-3
	Rate	0.6983	0.8016	0.8694	0.8782	
	After Extrapolation	3.8898e-3	1.6408e-3	5.8963e-4	1.8545e-4	5.3233e-5
	Rate	1.2453	1.4765	1.6688	1.8006	
2^{-14}	Before Extrapolation	1.5433e-2	9.6028e-3	5.5900e-3	3.0789e-3	1.6913e-3
	Rate	0.6845	0.7806	0.8604	0.8643	
	After Extrapolation	4.0459e-3	1.7118e-3	6.2066e-4	1.9732e-4	5.6955e-5
	Rate	1.2409	1.4636	1.6533	1.7926	
2^{-18}	Before Extrapolation	1.5485e-2	9.6442e-3	5.6179e-3	3.0960e-3	1.7018e-3
	Rate	0.6831	0.7796	0.8596	0.8633	
	After Extrapolation	4.0560e-3	1.7174e-3	6.2226e-4	1.9783e-4	5.7064e-5
	Rate	1.2398	1.4646	1.6533	1.7936	
2^{-20}	Before Extrapolation	1.5488e-2	9.6468e-3	5.6198e-3	3.0970e-3	1.7025e-3
	Rate	0.6830	0.7795	0.8597	0.8632	
	After Extrapolation	4.0565e-3	1.7177e-3	6.2234e-4	1.9785e-4	5.7068e-5
	Rate	1.2398	1.4647	1.6533	1.7937	
$e^{N,\Delta t}$	Before Extrapolation	1.5488e-2	9.6470e-3	5.6199e-3	3.0971e-3	1.7025e-3
$\rho^{N,\Delta t}$	Rate	0.6830	0.7795	0.8596	0.8633	
$e^{N,\Delta t}_{extr}$	After Extrapolation	4.0566e-3	1.7178e-3	6.2237e-4	1.9786e-4	5.7069e-5
$\rho^{N,\Delta t}_{extr}$	Rate	1.2398	1.4647	1.6533	1.7937	
Result in [22]						
$e^{N,\Delta t}$		1.021e-2	3.225e-3	1.066e-3	3.479e-4	1.111e-4
$\rho^{N,\Delta t}$		1.663	1.598	1.615	1.646	-

The computed maximum point-wise errors and the rate of convergence for Examples 1 and 2 are given in Tables 1 and 2, respectively. From these results, it is clear that the present method gives an ε-uniform convergence for Examples 1 and 2 before and after extrapolation. Comparison of Example 2 is given in Table 3. The computed maximum point-wise errors and the rate of convergence for Example 3 are given in Table 4 with its comparison. Numerical simulations for Examples 1 and 2 are plotted in Figure 1 and Example 3 in Figure 2. The maximum point-wise errors for Examples 1, 2, and 3 are plotted using log-log scale, as can be seen in Figures 3, 4, and 5, respectively. These figures clearly show that Richardson extrapolation increases the rate of convergence of the upwind scheme from $O(N^{-1} \ln N + \Delta t)$ to $O(N^{-2} \ln^2 N + \Delta t^2)$. Figures 6 and 7 show the effect of the perturbation parameter ε in terms of line graphs for Examples 1, 2, and 3. The effect of the singular perturbation parameter on the boundary layer of the solution for all Examples is shown in Figures 6 and 7. As observed in these Figures, as $\varepsilon \to 0$ strong boundary layer is formed near $x = 1$. The effect of the time level t in terms of line graphs for Examples 1, 2, and 3 is given in Figures 8 and 9. As observed from Figures 8 and 9, a strong boundary layer is formed near $x = 1$, and as the size of the time level increases, the thickness of the layer increases.

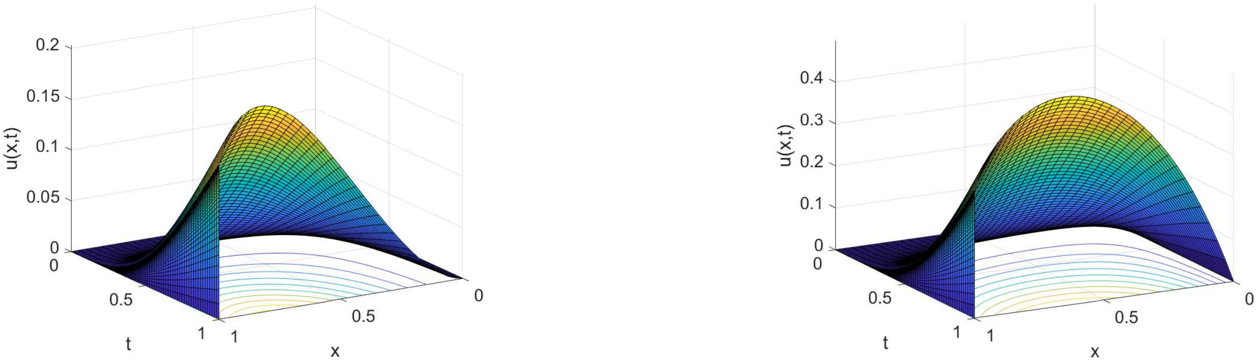

(a) Example 1 when $\mu = 0$ (b) Example 2 when $\mu = 0.3\varepsilon$

Figure 1. Surface plot of the numerical solution for $N = 64 = M$ and $\varepsilon = 10^{-6}$

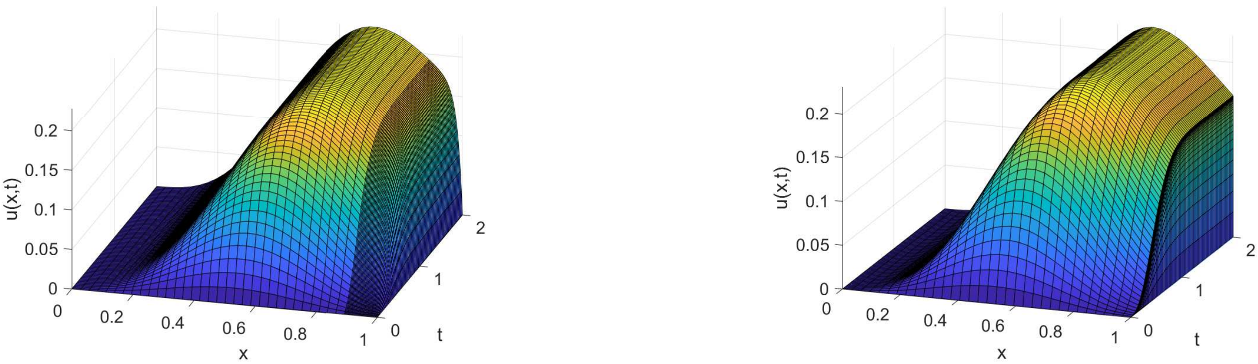

(a) At $N = 64, M = 80$ and $\varepsilon = 2^{-6}$ (b) At $N = 64, M = 80$ and $\varepsilon = 2^{-16}$

Figure 2. Surface plot of the numerical solution for Example 3 for $\mu = 0$

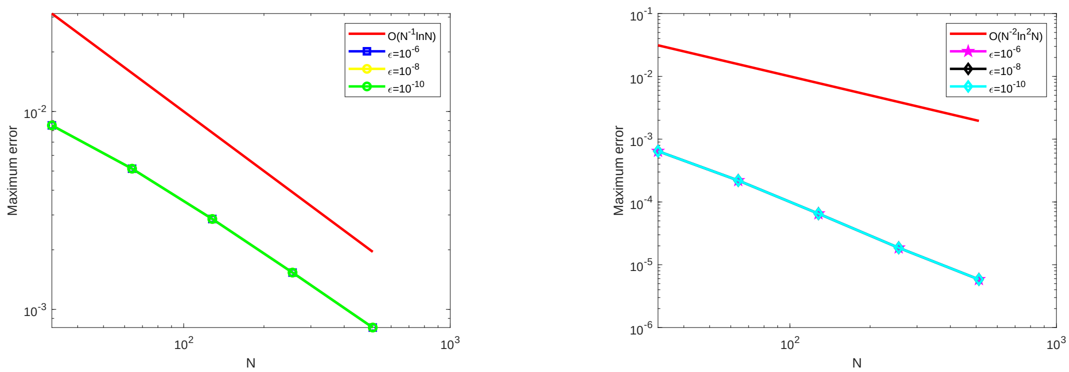

(a) Before extrapolation (b) After extrapolation

Figure 3. Log-log plot of the maximum point-wise errors at $\mu = 0$ for Example 1

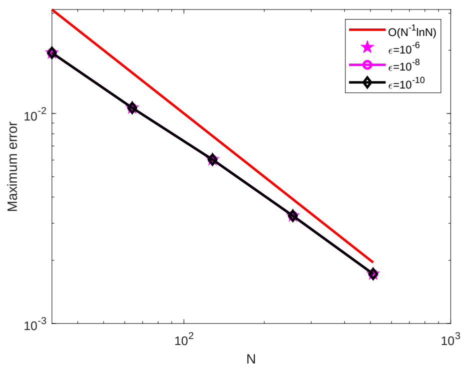

(a) Before extrapolation

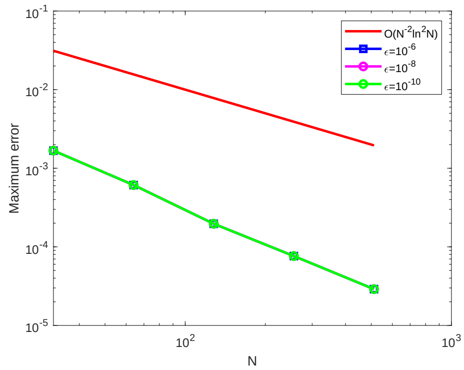

(b) After extrapolation

Figure 4. Log-log plot of the maximum point-wise errors at $\mu = 0.3\varepsilon$ for Example 2

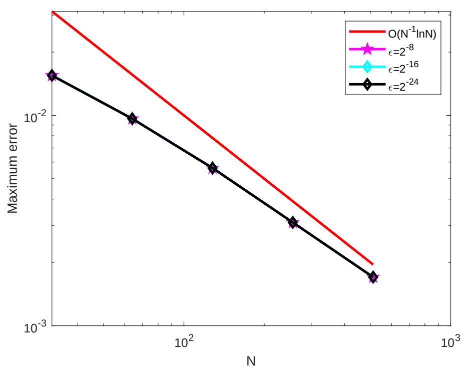

(a) Before extrapolation

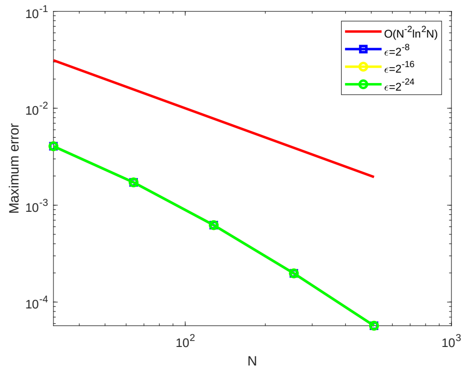

(b) After extrapolation

Figure 5. Log-log plot of the maximum point-wise errors at $\mu = 0$ for Example 3

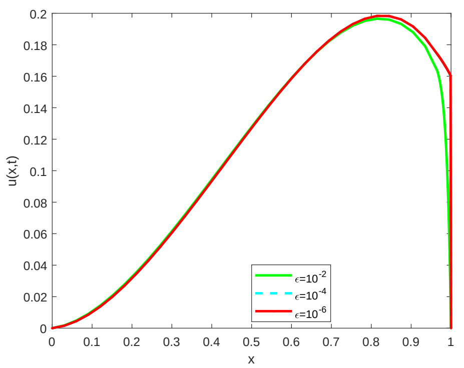

(a) Example 1 at $N = 64 = M$, $\mu = 0$

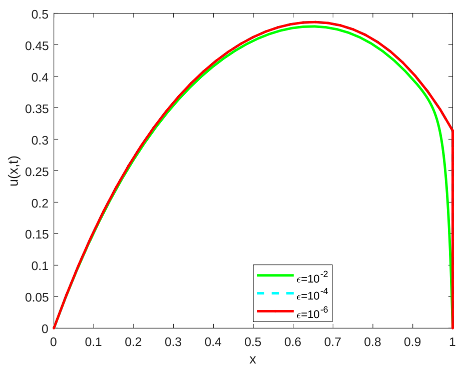

(b) Example 2 at $N = 64 = M$, $\mu = 0.3\varepsilon$

Figure 6. Effect of the perturbation parameter ε on the numerical solution

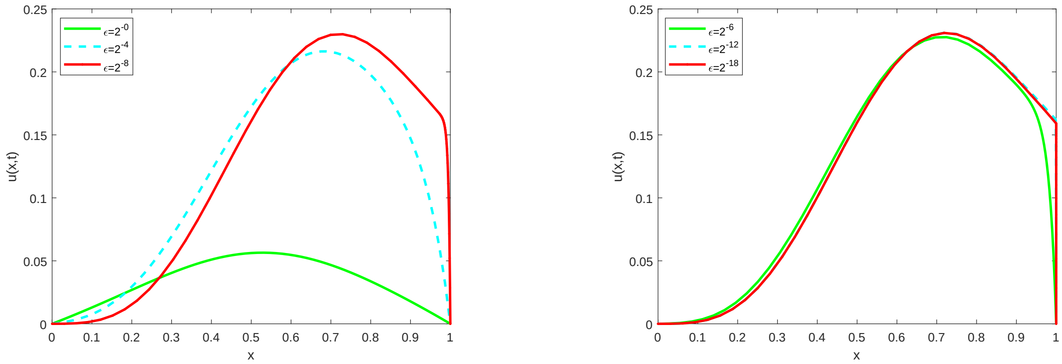

(a) At $N = 64, M = 80$, $\mu = 0$ (b) At $N = 64, M = 80$, $\mu = 0$

Figure 7. Effect of the parameter ε on the solution for Example 3

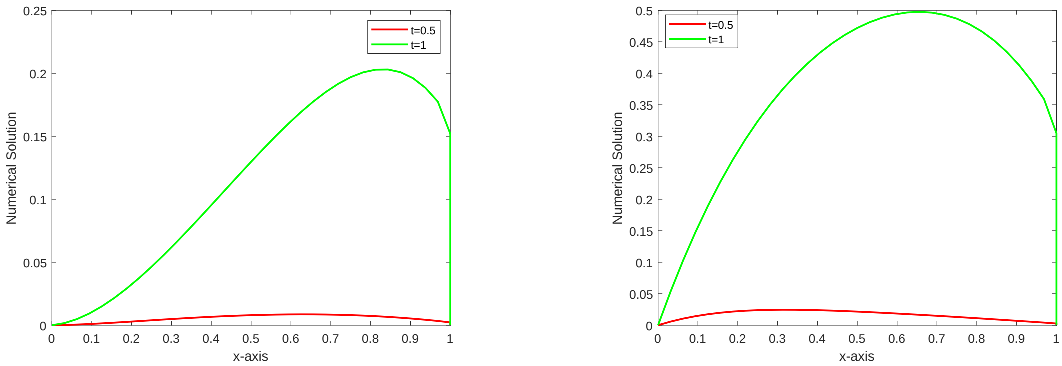

(a) Example 1 at $N = 64 = M$, $\varepsilon = 10^{-6}$, $\mu = 0$ (b) Example 2 at $N = 64 = M$, $\varepsilon = 10^{-6}$, $\mu = 0.3\varepsilon$

Figure 8. Effect of time t level on the solution

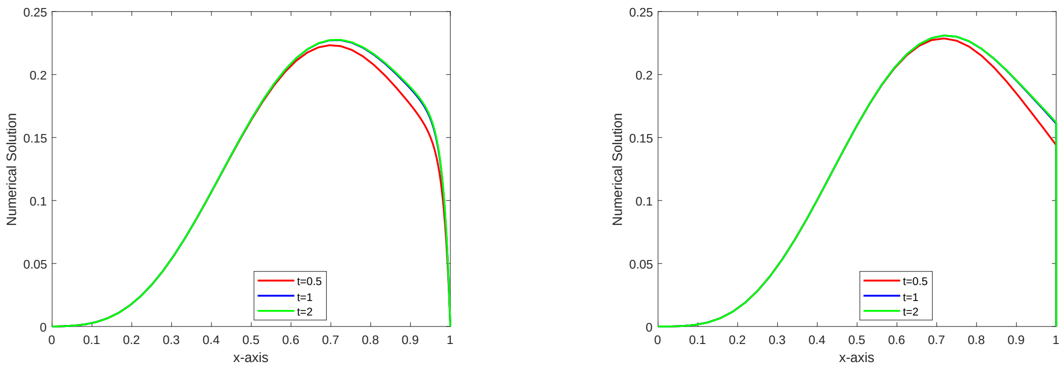

(a) At $N = 64, M = 80$, $\varepsilon = 2^{-6}$, $\mu = 0$ (b) At $N = 64, M = 80$, $\varepsilon = 2^{-16}$, $\mu = 0$

Figure 9. Effect of time t level on the solution interms of line graph for Example 3

Conclusion

This study presents a computational method that is almost second-order convergent for singularly perturbed parabolic differential difference equations with negative shifts. The Taylor series approximation is used to estimate the terms that involve delays. An implicit Euler technique for the time direction on a uniform mesh and an upwind difference method on a Shishkin mesh in the space direction are used to discretise the resulting singularly perturbed parabolic convection-diffusion-reaction equation. The stability and uniform convergence of the proposed method are established very well. The proposed method gives almost first-order convergence both in the time and space variables. The Richardson extrapolation technique is then applied to accelerate the order of convergence of the method in the time and space variables. Theoretically, we have proved that the extrapolation provides almost second-order $\varepsilon-$uniform convergence. To validate the applicability of the proposed method, some numerical examples are computed for different values of the perturbation parameter and delay parameter.

Author Contributions

All authors contributed equally to this work.

Conflict of Interest

The authors declare no conflict of interest.

References

1 Bansal, K., & Sharma, K.K. (2017). Parameter uniform numerical scheme for time dependent singularly perturbed convection-diffusion-reaction problems with general shift arguments. *Numerical Algorithms, 75*, 113–145. https://doi.org/10.1007/s11075-016-0199-3

2 Kumar, D. (2018). An implicit scheme for singularly perturbed parabolic problem with retarded terms arising in computational neuroscience. *Numerical Methods in Partial Differential Equations, 34*(6), 1933–1952. https://doi.org/10.1002/num.22269

3 Nageshwar Rao, R., & Pramod Chakravarthy, P. (2019). Fitted numerical methods for singularly perturbed one-dimensional parabolic partial differential equations with small shifts arising in the modelling of neuronal variability. *Differential Equations and Dynamical Systems, 27*(1), 1–18. https://doi.org/10.1007/s12591-017-0363-9

4 Gupta, V., Kumar, M., & Kumar, S. (2018). Higher order numerical approximation for time-dependent singularly perturbed differential-difference convection-diffusion equations. *Numerical Methods in Partial Differential Equations, 34*(1), 357–380. https://doi.org/10.1002/num.22203

5 Pramod Chakravarthy, P., & Kumar, K. (2019). An adaptive mesh method for time dependent singularly perturbed differential-difference equations. *Nonlinear Engineering, 8*(1), 328–339. https://doi.org/10.1515/nleng-2018-0075

6 Ramesh, V.P., & Priyanga, B. (2021). Higher order uniformly convergent numerical algorithm for time-dependent singularly perturbed differential-difference equations. *Differential Equations and Dynamical Systems, 29*(2), 239–263. https://doi.org/10.1007/s12591-019-00452-4

7 Shivhare, M., Pramod Chakravarthy, P., Ramos, H., & Vigo-Aguiar, J. (2023). Quadratic B-spline collocation method for time dependent singularly perturbed differential-difference equation arising in the modeling of neuronal activity. *Numerical Methods in Partial Differential Equations, 39*(3), 1805–1826. https://doi.org/10.1002/num.22738

8 Daba, I.T., & Duressa, G.F. (2021). Extended cubic B-spline collocation method for singularly perturbed parabolic differential-difference equation arising in computational neuroscience. *International Journal of Numerical Method in Biomedical Engineering, 37*(2), e3418. https://doi.org/10.1002/cnm.3418

9 Daba, I.T., & Duressa, G.F. (2021). A hybrid numerical scheme for singularly perturbed parabolic differential-difference equations arising in the modeling of neuronal variability. *Computational and Mathematical Methods, 3*(1), e3418. https://doi.org/10.1002/cmm4.1178

10 Woldaregay, M.M., & Duressa, G.F. (2021). Uniformly convergent hybrid numerical method for singularly perturbed delay convection-diffusion problems. *International Journal of Differential Equations, 2021*, 654495. https://doi.org/10.1155/2021/6654495

11 Daba, I.T., & Duressa, G.F. (2022). Collocation method using artificial viscosity for time dependent singularly perturbed differential-difference equations. *Mathematics and Computer in Simulation, 192*(2), 201–220. https://doi.org/10.1016/j.matcom.2021.09.005

12 Daba, I.T., & Duressa, G.F. (2021). Hybrid algorithm for singularly perturbed delay parabolic partial differential equations. *Applications and Applied Mathematics: An International Journal, 16*(1), 397–416. https://digitalcommons.pvamu.edu/aam/vol16/iss1/21

13 Rathish Kumar, B.V., & Kumar, S. (2015). Convergence of three-step Taylor Galerkin finite element scheme based monotone Schwarz iterative method for singularly perturbed differential difference equation. *Numerical Functional Analysis and Optimization, 36*(8), 1029–1045. https://doi.org/10.1080/01630563.2015.1043372

14 Kumar, S., & Rathish Kumar, B.V. (2017). A domain decomposition Taylor Galerkin finite element approximation of a parabolic singularly perturbed differential equation. *Applied Mathematics and Computation, 293*, 508–522. https://doi.org/10.1016/j.amc.2016.08.031

15 Kumar, S., & Rathish Kumar, B.V. (2017). A finite element domain decomposition approximation for a semi-linear parabolic singularly perturbed differential equation. *International Journal of Nonlinear Sciences and Numerical Simulation, 18*(1), 41–55. https://doi.org/10.1515/ijnsns-2015-0156

16 Woldaregay, M.M., & Duressa, G.F. (2023). Almost second-order uniformly convergent numerical method for singularly perturbed convection-diffusion reaction equations with delay. *Applicable Analysis: An International Journal, 102*(2), 651–671. https://doi.org/10.1080/00036811.2021.1961756

17 Ghafli, A.A.A., Gelu, F.W., & Salman, H.J.A. (2025). A layer-adapted numerical method for singularly perturbed partial functional-differential equations. *Axioms, 14*, 362. https://doi.org/10.3390/axioms14050362

18 Salman, H.J.A., Gelu, F.W., & Ghafli, A.A.A. (2024). A fitted mesh robust numerical method and analysis for the singularly perturbed parabolic PDEs with a degenerate coefficient. *Results in Applied Mathematics, 24*(1), 100519. https://doi.org/10.1016/j.rinam.2024.100519

19 Daba, I.T., Melesse, W.G., Gelu, F.W., & Kebede, G.D. (2025). Numerical investigation of singularly perturbed time lag parabolic differential-difference equations. *Heliyon, 11*(1), e41215. https://doi.org/10.1016/j.heliyon.2024.e41215

20 Daba, I.T., Melesse, W.G., Gelu, F.W., & Kebede, G.D. (2025). A high-order numerical scheme for singularly perturbed parabolic time delay problem with two small parameters. *Research in Mathematics, 12*(1), 2463184. https://doi.org/10.1080/27684830.2025.2463184

21 Kellogg, R.B., & Tsan, A. (1978). Analysis of some differences approximations for a singular perturbation problem without turning point. *Mathematics of Computation, 32*(144), 1025–1039.

22 Clavero, C., Gracia, J.L., & Jorge, J.C. (2005). Higher order numerical methods for one dimen-

sional parabolic singularly perturbed problems with regular layers. *Numerical Methods in Partial Differential Equations, 21*(1), 149–169. https://doi.org/10.1002/num.20030

23 Mukherjee, K., & Natesan, S. (2011). Richardson extrapolation technique for singularly perturbed parabolic convection-diffusion problems. *Computing, 92*(1), 1–32. https://doi.org/10.1007/s00607-010-0126-8

24 Stynes, M., & Roos, H-G. (1997). The midpoint upwind scheme. *Applied Numerical Mathematics, 23*(3), 361–374. https://doi.org/10.1016/S0168-9274(96)00071-2

*Author Information**

Duba Bura Huka — Master of Science, Lecturer, Borana University, 19, Yabello, Ethiopia; e-mail: *dubura65@gmail.com*

Wondwosen Gebeyaw Melesse — Doctor of Mathematics, Associate Professor, Dean of College of Natural and Computational Sciences, Dilla University, 419, Dilla, Ethiopia; e-mail: *gwondwosen12@gmail.com*; https://orcid.org/0000-0001-5966-4985

Fasika Wondimu Gelu (*corresponding author*) — Doctor of Mathematics, Assistant Professor, Dilla University, 419, Dilla, Ethiopia; e-mail: *Fasikag@du.edu.et*; https://orcid.org/0000-0002-4693-9051

*Authors' names are presented in the order: first name, middle name, and last name.